ELSEVIER

Journal of Photochemistry and Photobiology A: Chemistry 110 (1997) 107–113

Journal of PHOTOCHEMISTRY AND PHOTOBIOLOGY A: CHEMISTRY

IR and UV laser-induced photolysis of 2-chloroethenylsilane

Marta Castillejo [a,*], Rebeca de Nalda [a], Mohamed Oujja [a], Luis Díaz [b], Magna Santos [b]

[a] *Instituto de Química Física Rocasolano, CSIC, Serrano 119, 28006 Madrid, Spain*

[b] *Instituto de Estructura de la Materia, CSIC, Serrano 121, 28006 Madrid, Spain*

Accepted 21 May 1997

Abstract

The laser-induced decomposition of 2-chloroethenylsilane was studied in the IR with a TEA CO_2 laser and in the UV with a narrow-band, frequency-doubled dye laser at 212.5 nm. Silylene was observed in the IR multiphoton dissociation (MPD) via laser-induced fluorescence (LIF). The nascent silylene fragments are vibrationally excited in the bending mode. Multiphoton UV photolysis yields a fluorescence emission spectrum originating from the SiH ($A^2\Delta \rightarrow X^2\Pi$) $\Delta v = 0$ system, with several atomic Si transitions and molecular bands corresponding to C_2 ($d^3\Pi_g \rightarrow a^3\Pi_u$) $\Delta v = 2, 1, 0, -1$ and -2 transitions. The simulation of the spectra originating from diatomic fragments indicates that these possess a high content of internal energy. A high population of Si triplet states is observed. © 1997 Elsevier Science S.A.

Keywords: 2-Chloroethenylsilane; IR; Laser-induced fluorescence; UV

1. Introduction

The laser-induced decomposition of 2-chloroethenylsilane (CES) has been shown to be promising for the chemical vapour deposition of silicon carbide [1]. The laser-induced photodecomposition of CES has been investigated recently using IR multiphoton dissociation (MPD), employing one or two CO_2 laser fields [2,3] and UV irradiation with an ArF laser [1]. As a result of these studies, two main decomposition pathways have been postulated

$$H_3Si\text{–}CH\,|CHCl \rightarrow H_3SiC{\equiv}CH + HCl$$

$$H_3Si\text{–}CH\,|CHCl \rightarrow H_2C\,|CHCl + SiH_2$$

$$H_3SiC{\equiv}CH \rightarrow HC{\equiv}CH + SiH_2$$

IR MPD studies of CES indicate that, for low fluence conditions (5 J cm^{-2} or less), the dominant dissociation reaction is dehydrochlorination, followed by the decomposition of ethynylsilane. UV photodissociation studies of CES have led to the characterization of the gaseous products formed during photolysis by Fourier transform IR (FTIR) spectroscopy and of the resulting solid deposits by several spectroscopic techniques [1]. These studies support the belief that dehydrochlorination is the most efficient primary photofragmentation pathway. Recently, other workers have detected and analysed the intense visible luminescence produced during the IR MPD of CES at high fluence conditions (5 J cm^{-2} or more) [2]. This emission has been assigned to the $A^1B_1 \rightarrow X^1A_1$ electronic transition of the silylene radical, formed within the laser pulse. The detection of silylene gives support to the previously postulated reaction pathways in the IR MPD of this molecule, and suggests that, at high fluence conditions, the chloroethene elimination channel dominates the dissociation reaction.

The work presented here represents another step in the general objective of correlating the properties of the gaseous products and solid deposits formed with the primary fragmentation channels available during the laser irradiation of CES. The fluorescence excitation spectrum of the $A^1B_1 \downarrow X^1A_1$ transition of the SiH_2 radical, produced during the IR MPD of CES with a TEA CO_2 laser, has been obtained. We have also analysed the spontaneous fluorescence emission resulting from the MPD of CES with a narrow-band, frequency-doubled dye laser at 212.5 nm. The results of this study shed light on the mechanisms participating in the production of the observed photofragments and on the relative importance of the primary photodissociation channels of the molecule.

2. Experimental details

Two different experimental systems have been used in this work. The experimental set-up for laser-induced fluorescence

* Corresponding author.

PII S1010-6030(97)00172-X

(LIF) studies in the IR MPD of CES has been described in part in Ref. [2]. IR photolysis was carried out with a Lumonics K-103 CO_2 laser using the 10R(28) line at 936.8 cm^{-1}, nearly coincident with the SiH_3 mode of CES [3]. The laser operates with a mixture of CO_2, NO_2 and He in the proportion 8 : 8 : 84, the pulse temporal profile being monitored with a photon drag detector (Rofin Sinar 7415). The measured laser pulse consists of a spike of 85 ns (full width at half-maximum, FWHM) followed by a tail of around 3 μs. Experiments were performed in a static Pyrex cell fitted with a pair of NaCl windows orthogonal to another pair of quartz windows. The pressures of the samples of CES diluted in Ar were measured in the cell with a capacitance manometer (MKS Baratron, 0–0.75 Torr). An IR laser fluence of 5 J cm^{-2} was obtained by focusing the CO_2 laser at the centre of the cell using an NaCl lens with a focal length of 10 cm. Fluorescence was induced in the nascent fragments using an N_2-pumped dye laser (PRA LN107) with a bandwidth of 1.2 cm^{-1} at 580 nm. The dye laser, collinear and counterpropagating to the CO_2 laser, was focused by a 50 cm quartz lens at the centre of the photolysis region. The delay between the CO_2 and probe laser was controlled by a Berkeley Nucleonics (BNC 7036A) unit to within ±50 ns. Total LIF was detected through one of the quartz windows perpendicular to the laser axis and focused onto an R928 Hamamatsu photomultiplier through a Schott RG610 glass filter. Photomultiplier signals were sent to a Tektronix TDS540 digital oscilloscope on line with a personal computer, where they were averaged and analysed.

The experimental set-up for UV photofragmentation studies has been described recently [4], and a short summary will be given here. Photolysis radiation was obtained by frequency doubling in a BBO crystal cut at 81° to the output of a home-built dye laser pumped by an XeCl excimer laser. The frequency-doubled laser delivered around 0.1 mJ of 212.5 nm polarized light with a bandwidth of 0.4 cm^{-1} in pulses of 15 ns. The photolysis beam at 212.5 nm was focused by a lens with a focal length of 15 cm in the centre of a glass cell fitted with quartz windows. The pressures of the CES samples, ranging from 100 to 300 mTorr, were measured with a capacitance manometer with the same characteristics as that used in the IR experiments. The cell was connected to a glass vacuum system, routinely operating at a vacuum of 10^{-5} Torr. The detection of photofragment emission was made perpendicular to the photolysis beam by an EMI 9816 QB photomultiplier. Spectral selection was performed by a 0.5 m Spektronik monochromator. When needed, cut-off filters were used in certain experiments to avoid contamination of the signal with second orders of short-wavelength radiation. The electric signal generated in the photomultiplier was either viewed directly on a 40 MHz digital oscilloscope (Tektronix 2430A) or fed into a boxcar averager (SR250) interfaced with a personal computer for subsequent data analysis.

The preparation of CES followed the chemical procedure given elsewhere [1,2]. CES was obtained as a mixture of the cis and trans isomers (cis : trans, 1 : 3). The purity of the CES sample was checked by gas chromatography to be approximately 95%. The Ar purity was 99.998%.

3. Results

3.1. LIF studies during IR MPD

A LIF spectrum of the photofragments resulting from the IR MPD of CES was recorded by scanning the probe laser in the region between 574.5 and 597.0 nm in steps of 0.2 nm. The temporal behaviour of the LIF signal at each wavelength shows a contribution corresponding to the scattering of the dye laser on the windows of the cell, which disappears after the first 40 ns. For longer times, the temporal profile can be fitted to a single exponential function with decay times between 200 and 300 ns. Therefore the intensity of the LIF signal at each wavelength is estimated by integration in a temporal window from 40 to 400 ns; fitting to an exponential function provides information about the decay time of the set of excited states contributing to the emission. Fig. 1 shows the LIF spectrum recorded at two different probe to pump delay times of 600 ns and 5 μs. The sample contained 75 mTorr of CES in 750 mTorr of Ar, the pressure of Ar buffer gas being chosen to maximize the intensity of the signal. Each point in the spectrum was obtained by averaging the signal over 20 laser shots. Before averaging, each signal was normalized for variations in the energy of the dissociating and probe lasers. Every 200 laser shots, the cell was filled with fresh sample to avoid the buildup of photolysis products that could disturb the LIF signal. The time between IR pulses exceeds 30 s, which appears to be long enough for the solid particles to settle and for the gaseous products to diffuse out of the reaction zone. The spectrum in Fig. 1 consists of four broad bands superimposed on a background. These features may be due to hot band absorption, the bandwidth of the visible probe laser and the amplified spontaneous emission (ASE) present in the dye laser output. The four bands are

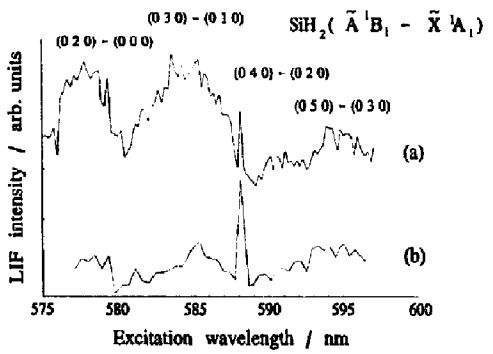

Fig. 1. LIF spectrum following IR MPD of a mixture of 75 mTorr of CES in 750 mTorr of Ar. The scan step is 0.2 nm. The assignment of the SiH_2 $^1B_1(0,v_2,0) \downarrow {}^1A_1(0,v_1,0)$ transitions is indicated. The delay between the photolysis and probe laser is 600 ns (a) and 5 μs (b).

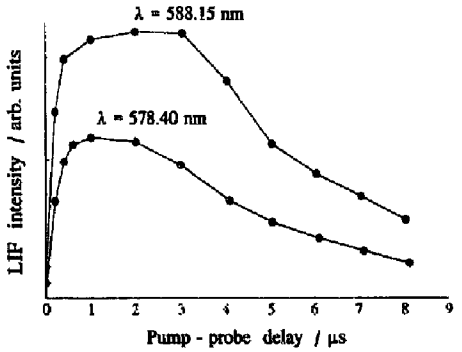

Fig. 2. Timescale of the LIF signal in the IR MPD of 75 mTorr of CES in 750 mTorr of Ar, monitored by the dependence of the intensity at 578.40 and 588.15 nm on the time delay between the IR and visible laser.

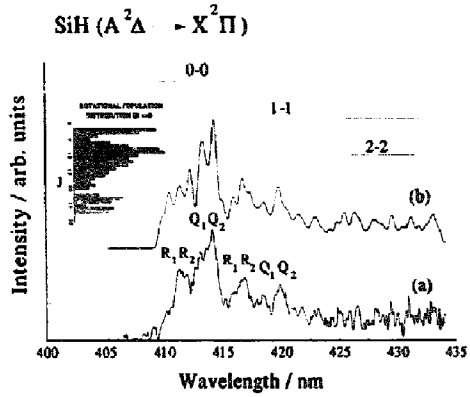

Fig. 3. (a) Fluorescence emission spectrum from SiH ($A^2\Delta \rightarrow X^2\Pi$) $\Delta v = 0$ obtained by photolysis of 150 mTorr of CES at 212.5 nm. The spectral resolution is 5 Å. (b) Simulated spectrum obtained using the TSVD method. The inset shows the rotational population distribution for $v' = 0$.

readily assigned to SiH_2 $^1B_1(0,v_2,0) \leftarrow {}^1A_1(0,v_1,0)$ transitions with $\Delta v = v_2 - v_1 = 2$ [5,6]. In the present experimental conditions, it was not possible to resolve the rotational structure of the vibronic transitions. According to the calculated Franck–Condon factors for these transitions [6], it appears that most of the population of the nascent SiH_2 fragments is produced in vibrationally hot form. The spectrum taken at a longer delay, 5 μs after the IR photolysis pulse, shows a considerable reduction in intensity of the bands, except for the line observed at 588.15 nm. The intensity of this line remains practically unchanged with increasing time delay. Similar effects have been reported in LIF studies following the IR MPD of certain organosilanes [7,8], and have been explained by the effect of extensive rotational cooling, induced by collisions with the buffer gas, which leads to the accumulation of the nascent rotational population in a selected set of states.

We studied the dependence of the LIF signal on the time delay between the photolysis and probe lasers. Fig. 2 shows the LIF signal corresponding to the excitation of the SiH_2 fragment at two wavelengths (578.40 and 588.15 nm) as a function of this delay. Both signals reach a maximum value within 1 μs after the CO_2 laser pulse. From this rapid rise, it seems that SiH_2 production takes place during the IR pulse. The signal recorded at 588.15 nm maintains its maximum intensity during a longer time than the signal at 578.40 nm, probably reflecting the timescale for rotational cooling. The LIF signals decay with a tail of several microseconds. For the pressure conditions applied, the observed decay time may contain contributions from both spontaneous diffusion of the radicals out of the volume probed by the excitation pulse and reaction of the SiH_2 radical with the parent or other decomposition products.

3.2. *Photofragment emission during photolysis at 212.5 nm*

Photofragment emission spectra were recorded in the region from 200 to 700 nm. The most intense emission produced during the UV photolysis of CES at 212.5 nm was observed in the wavelength interval of 400–430 nm and assigned to the $A^2\Delta \rightarrow X^2\Pi$ $\Delta v = 0$ transition of the SiH fragment. The spectrum is presented in Fig. 3, together with the assignment, showing contributions from vibrational transitions $v'-v'' = 0$–0, 1–1 and 2–2. The rovibrational populations giving rise to the observed emissions were estimated by a computer program based on a truncated singular value decomposition (TSVD) method [9]. The resulting ratio of vibrational population in level $v' = 1$ relative to $v' = 0$ was 0.75 ± 0.05. However, the relative population of $v' = 2$ was subject to very high uncertainties due to the low intensity of the 2–2 band. The rotational population distribution of $v' = 0$ is presented in the inset of Fig. 3. Two regions, the first between $J' = 8$ and $J' = 15$ and the other centred at $J' = 25$, seem to locate most of the population of the state, producing a distribution far from equilibrium. The calculated average rotational energy in the $v' = 0$ level is 1560 ± 200 cm^{-1}. The determination of the rotational populations for $v' = 1$ and $v' = 2$ is less clear due to strong overlapping of the bands in the regions in which these levels contribute to the emission. The calculated spectrum is also shown in Fig. 3. It is of interest to compare the SiH (A) spectrum and the corresponding rovibrational population distribution obtained by photolysis of CES with those obtained during the photolysis of phenylsilane at the same wavelength [4]. For phenylsilane, the retrieved population distribution in $v' = 0$ also presents a bimodal structure, and the resulting ratio of the vibrational populations in levels $v' = 1$ and $v' = 0$ is 0.6 ± 0.1, very close to the value of 0.75 ± 0.05 obtained for CES.

In the range between 200 and 300 nm, five atomic Si emission lines, from two triplet and three singlet excited states, are observed. Fig. 4 depicts the spectrum in this region and the assigned transitions. Due to the enhancement of the grating efficiency at 500 nm, the transition $3d^1D_2^0 \rightarrow 3p^1D_2$, at 243.5 nm, not present in the spectral region of Fig. 4, is observed in second order. The triplet structure of the

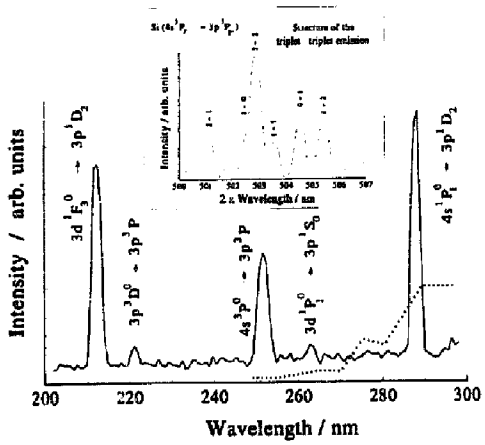

Fig. 4. Atomic Si emission spectrum resulting from the 212.5 nm photodissociation of 150 mTorr of CES. The spectral resolution is 30 Å and 5 Å for the spectrum in the inset, where one triplet emission is resolved in second order. The dotted line shows the efficiency of the detection system as a function of wavelength.

$4s^3P^0 \rightarrow 3p^3P$ transition, as shown in Fig. 4, is resolved by observing it in second order. Individual lines $J' \rightarrow J''$ of $2 \rightarrow 1$, $1 \rightarrow 0$, $2 \rightarrow 2$, $1 \rightarrow 1$, $0 \rightarrow 1$ and $1 \rightarrow 2$ are assigned.

Once the relative intensities of the observed lines have been corrected for the system response, an estimate of the relative populations of the upper states can be made using the expression

$$N = \left(\frac{g_u}{g_l}\right)\frac{I}{f}\lambda^2$$

where N is the population of the upper level, g_u and g_l are the degeneracies of the upper and lower states respectively, I and λ are the intensity and wavelength of the observed line respectively and f is the oscillator strength of the corresponding transition. Values of f were taken from the literature [10]. It is interesting to compare the populations of the $4s^3P^0$ and $4s^1P_1^0$ states, which have similar energies. The populations of the J' sublevels in the $4s^3P^0$ state are assumed to be proportional to their degeneracy; this assumption is supported by the analysis of the relative intensities of the different lines in the resolved triplet–triplet transition. The resulting ratio between the populations of the $4s^3P^0$ and $4s^1P_1^0$ states is ten. It seems, therefore, that the dissociation process favours, to some extent, the production of triplet states. We have compared the observed distribution of excited silicon states with that obtained in the MPD of phenylsilane at 212.5 nm [4]. In the photolysis of CES, the intensity of the lines arising from excited triplet states relative to the intensity corresponding to singlet states is substantially higher than in phenylsilane.

A series of five intense bands was detected in the region of 420–625 nm; these were assigned to the Swan bands of the carbon molecule C_2 ($d^3\Pi_g \rightarrow a^3\Pi_u$) $\Delta v = 2, 1, 0, -1$ and -2. The spectrum covering the full region is shown in Fig. 5. Fig. 6 shows the $\Delta v = 1$ band with higher resolution. Emissions from vibrational levels v' in the upper electronic state

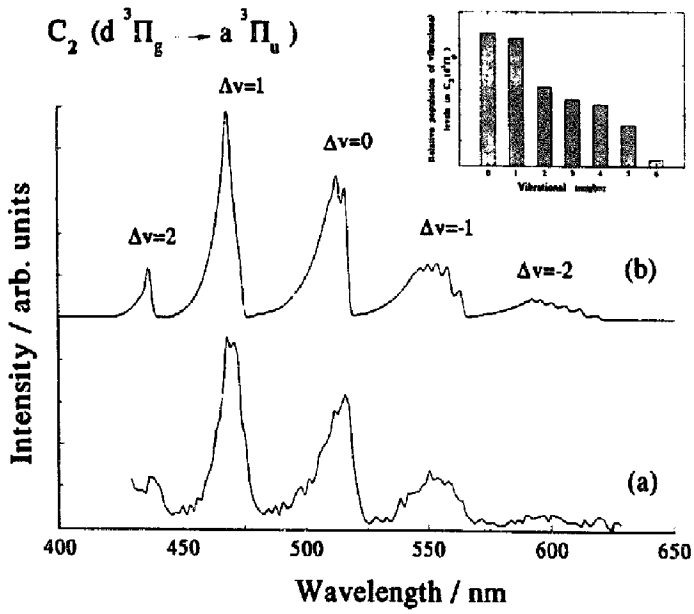

Fig. 5. (a) Swan bands of C_2 produced in the 212.5 nm photodissociation of 150 mTorr of CES with a resolution of 25 Å. A tail of the SiH ($A^2\Delta \rightarrow X^2\Pi$) emission is superimposed on the region of the $\Delta v = 2$ band. (b) Simulated spectrum calculated by assuming $T_{ROT} = 5500$ K and the vibrational distribution shown in the inset (see text).

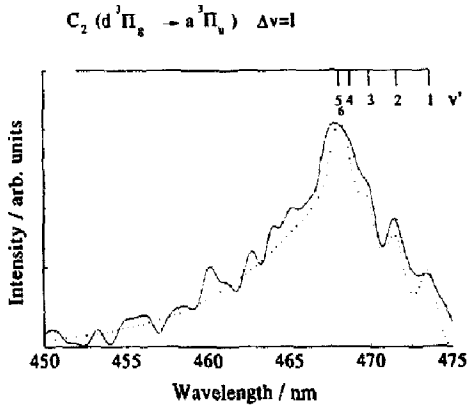

Fig. 6. Spectrum of the $\Delta v = 1$ band of the C_2 Swan system resulting from the photodissociation of 150 mTorr of CES at 212.5 nm taken with a resolution of 10 Å. The full line represents the experimental spectrum and the dotted line the corresponding simulation, which was performed with the rovibrational distribution of 5.

up to $v' = 6$ were assigned. The very high rotational levels of the C_2 (d) state contribute to the observed spectrum; this leads to the extremely strong overlap of many different lines, which, together with the limited spectral resolution, forbids definitive conclusions from being reached about the individual populations of the rovibrational levels. Thus a modification was introduced in the computer simulation program, so that the only unknown parameters were the relative vibrational populations in the $d^3\Pi_g$ state. By assuming rotational equilibrium in each vibrational level, the best rotational temperature for all substantially populated states was found by trial and error to be 5500 ± 400 K. The relative vibrational populations provided by the simulation for $v' = 0$–6 are 1/0.96/0.60/0.50/0.46/0.31/0.05, with errors within 10% of the given values. The corresponding average vibrational energy is 3200 ± 500 cm^{-1}. Fig. 5 and Fig. 6 also show the resulting calculated spectra.

The dependence of the observed emissions on the laser energy is shown in Fig. 7. The fluorescence originating from the SiH ($A^2\Delta \rightarrow X^2\Pi$) $\Delta v = 0$ transition is linearly dependent on the laser energy; this is shown in Fig. 7(a). The dependence of the Si atomic emissions was determined for several lines. Fig. 7(b) presents the results corresponding to the Si ($4s^3P^0 \rightarrow 3p^3P$) transition; the slope of the logarithmic plot gives a value of 2.4 ± 0.1. Other lines corresponding to $3d^1F_3^0 \rightarrow 3p^1D_2$ and $4s^1P_1^0 \rightarrow 3p^1D_2$ transitions yield similar slopes. Finally, the dependence of the C_2 ($d^3\Pi_g \rightarrow a^3\Pi_u$) emission on the laser energy was measured in the $\Delta v = 1$ band and found to be quadratic, as shown in Fig. 7(c).

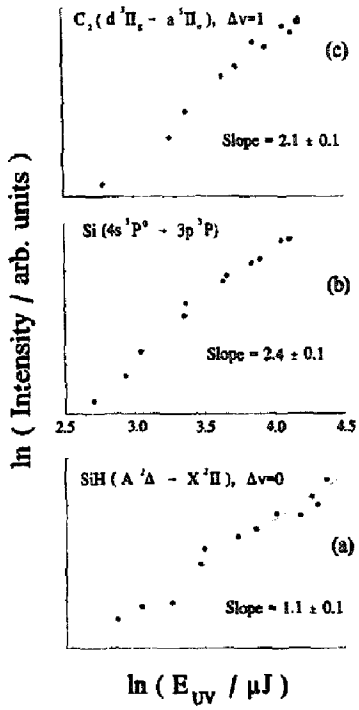

Fig. 7. Logarithmic plots of the dependence on laser energy of the observed photofragment emissions resulting from the photolysis of CES at 212.5 nm: (a) SiH ($A^2\Delta \rightarrow X^2\Pi$), $\Delta v = 0$ at 413 nm; (b) Si ($4s^3P^0 \rightarrow 3p^3P$) at 252 nm; (c) C_2 ($d^3\Pi_g \rightarrow a^3\Pi_u$), $\Delta v = 1$ at 470 nm. The slopes of the linear regression fits were 1.1 ± 0.1, 2.4 ± 0.1 and 2.1 ± 0.1 respectively.

4. Discussion

In this work, SiH_2 ($^1A_1$) has been identified in the IR MPD of CES by studying the fluorescence excitation spectrum of its $^1B_1(0,v_2,0) \leftarrow {}^1A_1(0,v_1,0)$ transitions. The behaviour of the LIF signal as a function of the probe to pump delay indicates that this radical is produced only in the presence of the IR pulse, and hence by photolysis not via secondary chemistry. This result leads to the conclusion that the SiH_2 radical is actually produced in the dissociation process and provides confirmation of the postulated primary routes, i.e. secondary photolysis of ethynylsilane formed via dehydrochlorination or chloroethene elimination. Previous studies [3] have shown that dehydrochlorination, having a lower activation energy, is favoured at the fluence of 5 J cm^{-2} used in this experiment. However, the LIF spectrum obtained in this work does not provide information on the relative importance of the two possible silylene-producing channels.

More information regarding the fate of this SiH_2 fragment can be obtained by discussing the results found in the present work when dissociation of the parent molecule was carried out in the UV spectral region. We consider the possible mechanisms participating in the formation of the electronically excited photofragments during MPD of CES at 212.5 nm and the role played by SiH_2 as a possible precursor of Si-containing fragments. We consider that the observed photofragments are formed through multistep processes involving interme-

diate species originating in the primary decomposition channels

$$H_3Si\text{–}CH\,|CHCl \rightarrow H_3SiC{\equiv}CH + HCl$$

$$\Delta H_0^0 = 8300\ cm^{-1} \quad (1)$$

$$H_3Si\text{–}CH\,|CHCl \rightarrow H_2C\,|CHCl + SiH_2$$

$$\Delta H_0^0 = 20\,460\ cm^{-1} \quad (2)$$

These intermediate species will suffer dissociation after subsequent photon absorption within the laser pulse, giving rise to the final fragments. To carry out the indicated energy balance, the heat of formation of CES is needed. Due to the lack of experimental determinations, its value has been estimated from that of ethenylsilane as 5350 cm^{-1} [11]. The silicon-containing fragments, i.e. the SiH (A) radical and the excited silicon atoms, may have their origin in the intermediates $H_3SiC{\equiv}CH$ or SiH_2 formed via processes (1) and (2) respectively.

The production of the SiH (A) radical may be connected with the appearance of the SiH_2 intermediate, formed in primary process (2) or in the decomposition of ethynylsilane. The various mechanisms leading to the dissociation of ethynylsilane have been investigated by ab initio molecular orbital methods [12]. The pathway leading to a transient species, which dissociates without a barrier to the products C_2H_2 and SiH_2

$$H_3SiC{\equiv}CH \rightarrow HC{\equiv}CH + SiH_2$$

$$\Delta H_0^0 = 20\,430\ cm^{-1} \quad (3)$$

is preferred energetically and kinetically. This theoretical prediction seems to be confirmed by the results obtained in the 193.3 nm photolysis of this compound, which produces high yields of C_2H_2 gaseous product [1]. According to Ref. [12], ethynylsilane can decompose to yield SiH_2 by several other routes, but these require more energy. The SiH_2 intermediate, formed by the two pathways suggested above, will photodissociate after subsequent photon absorption to yield the SiH fragment via the process

$$SiH_2\,(X^1A_1) \rightarrow H\,(^2S_g) + SiH\,(A^2\Delta)$$

$$\Delta H_0^0 = 51\,213\ cm^{-1} \quad (4)$$

The calculation of the potential energy surface of the silylene system has allowed the dissociation channels in the different excited states to be determined [13]. Two SiH_2 singlet excited states $^1A_2$ and $^1A_1$ at 4.745 and 5.532 eV respectively correlate with the dissociation channel (4). Therefore SiH (A) can be produced by two possible mechanisms. The path that requires less energy includes two steps corresponding to processes (2) and (4). The alternative mechanism consists of the sequence of processes (1), (3) and (4). As noted above, the rovibrational population distribution of SiH (A), resulting from the MPD of CES, is very similar to that obtained in the MPD of phenylsilane at the same wavelength. One of the identified primary decomposition channels of phenylsilane yields SiH_2, and this radical has been suggested as a possible precursor for the observed SiH emission [4]. The similarity of the population distributions may indicate that the mechanism in which SiH ($A^2\Delta$) is formed becomes, at some stage of the absorption process, independent of the parent molecule, and gives an argument in favour of the two-step process. A common SiH_2 intermediate species, formed in primary process (2), would undergo further absorption and dissociation through process (4), ultimately leading to SiH (A). The required energy to produce the SiH (A) fragment from CES corresponds to the absorption of at least two photons of 212.5 nm. Therefore the observed linear dependence on the laser energy may indicate the saturation of one of the absorption steps participating in the process. The laser fluence used in these experiments is around $F = 5 \times 10^{18}$ photons cm^{-2}. As the absorption cross-section of CES at 212.5 nm is $\sigma \approx 2 \times 10^{-18}\ cm^2$, measured in a Cary 3E UV–visible spectrophotometer, $\sigma F > 1$, indicating that the first absorption step is most probably saturated.

As noted above, SiH_2, formed via process (2) or (3), could be invoked as a precursor of atomic silicon fragments. However, a lower energy route for the production of excited Si atoms involves the dissociation of ethynylsilane via the two-step process [12]

$$H_3SiC{\equiv}CH \rightarrow HC{\equiv}CSiH + H_2$$

$$\Delta H_0^0 = 16\,100\ cm^{-1} \quad (5a)$$

$$HC{\equiv}CSiH \rightarrow C_2H_2 + Si$$

$$\Delta H_0^0 = 26\,110\ cm^{-1} \quad (5b)$$

The formation of excited silicon atoms via this pathway requires at least three laser photons. The observed quadratic dependence of the atomic silicon emission on the laser energy could be explained (as for SiH (A)) if saturation of the first absorption step involving the parent molecule takes place. In this case, the comparison between the MPD experiments of CES and phenylsilane [4] provides an argument against SiH_2 as the precursor of the atomic fragments. The distribution of the population between silicon excited states shows, in the case of CES, a higher preference for triplet states, which cannot be explained if a common SiH_2 precursor is invoked. This argument, together with energetic considerations, favours the pathway in which process (1) is followed by process (5) as the origin of the atomic fragments. For such a pathway, the high yield of excited triplet silicon states, in the case of CES, could indicate that dissociation of the intermediate $HC{\equiv}CSiH$ gives rise to fragments in triplet electronic states with high yield.

Similarly, the observed C_2 ($d^3\Pi_g$) fragment may have its origin in one of the primary products of the photodissociation of CES; these are ethynylsilane and chloroethene produced via processes (1) and (2) respectively. The photolysis of chloroethene at 212.5 nm yields C_2 ($d^3\Pi_g$), as demonstrated by the observation of the Swan bands [14]. However, we have compared the intensity of the Swan bands produced by

photolysis, under identical experimental conditions, of the same pressures of CES and chloroethene. We found that the intensity is around ten times higher for CES, indicating that this molecule is more efficient than chloroethene in producing C_2 ($d^3\Pi_g$) radicals. This result provides an argument against chloroethene as the precursor of excited diatomic carbon molecules which, alternatively, could be formed via the participation of the intermediate ethynylsilane.

5. Conclusions

The LIF spectrum of the fragments produced during the IR MPD of CES can be attributed to the SiH_2 radical, which is produced during the dissociation process. The spectrum indicates that the nascent SiH_2 fragments are vibrationally excited, at least in the bending mode. The results of the MPD experiments at 212.5 nm indicate the participation of this radical as an intermediate in the production of the SiH (A) photofragment. Arguments based on energetic considerations and on the similarity of the rovibrational distributions of SiH (A) produced in the 212.5 nm photolysis of CES and phenylsilane support this assumption. A similar type of argument favours ethynylsilane as an intermediate in the production of Si atomic fragments. Finally, the high yield of C_2 ($d^3\Pi_g$) emission, compared with that obtained in the photolysis of chloroethene at the same wavelength, rules out the participation of this species as an intermediate in the production of the diatomic carbon fragment.

Acknowledgements

The authors wish to acknowledge Dr J. Pola for useful discussions and for providing the CES sample. We also thank Dr R. Becerra for estimating the heat of formation of CES and determining the sample purity and Dr P. Lillo for measuring the CES absorption spectrum. This work was financed by DGYCYT (PB93-0145-C02-01/02) and by the HCM Programme (CHRX-CT94-0485). R. de Nalda thanks MEC for a scholarship.

References

[1] J. Pola, Z. Bastl, J. Subrt, J.R. Abeysinghe, R. Taylor, J. Mater. Chem. 6 (1996) 155.
[2] M. Santos, L. Díaz, J.A. Torresano, J. Pola, J. Photochem. Photobiol. A: Chem., in press.
[3] M. Santos, L. Díaz, Z. Bastl, V. Hulínký, M. Urbanová, J. Váek, J. Pola, J. Mater. Chem. 6 (1996) 975.
[4] M. Oujja, M. Martín, R. de Nalda, M. Castillejo, Laser Chem. 16 (1996) 157.
[5] M. Fukushima, S. Mayama, K. Obi, J. Chem. Phys. 96 (1992) 44.
[6] G. Duxbury, A. Alijah, R.R. Trieling, J. Chem. Phys. 98 (1993) 811.
[7] J.W. Thoman Jr., J.I. Steinfeld, Chem. Phys. Lett. 124 (1986) 35.
[8] D.M. Rayner, R.P. Steer, P.A. Hackett, C.L. Wilson, P. John, Chem. Phys. Lett. 123 (1986) 449.
[9] J. Ruiz, M. Martín, Comput. Chem. 19 (1995) 417.
[10] W.L. Wiese, G.A. Martin, Wavelengths and Transition Probabilities for Atoms and Atomic Ions. Part II: Transition Probabilities, US Government Printing Office, Washington DC, 1980.
[11] N. Al-Rubaiey, R. Walsh, J. Phys. Chem. 98 (1994) 5303.
[12] J.S. Francisco, C. Kurz, J.J.W. McDouall, Chem. Phys. Lett. 162 (1989) 79.
[13] C. Winter, P. Millie, Chem. Phys. 174 (1993) 177.
[14] M. Oujja, J. Ruiz, R. de Nalda, M. Castillejo, Laser Chem. 16 (1996) 207.